

Enhanced uplink non-orthogonal multiple access for 5G and beyond systems

Wen-jia LIU[‡], Xiao-lin HOU, Lan CHEN

DOCOMO Beijing Communications Laboratories Co., Ltd., Beijing 100190, China

E-mail: liuwj@docomolabs-beijing.com.cn; hou@docomolabs-beijing.com.cn; chen@docomolabs-beijing.com.cn

Received Dec. 15, 2017; Revision accepted Feb. 27, 2018; Crosschecked Mar. 20, 2018

Abstract: Uplink non-orthogonal multiple access (NOMA) is a promising technique to meet the requirements of the fifth generation (5G) and beyond systems. Various NOMA schemes have been proposed in both academia and industry. However, most existing schemes assume equal average received power, which limits the performance. We propose three enhancements of uplink NOMA to achieve the requirements of massive connectivity and high reliability in 5G, where unequal average received power is exploited as part of the multiple access signature. First, the optimal sequences targeting to generalized Welch-bound equality (GWBE) are obtained for unequal average received power. Then user grouping with multi-level received powers is proposed for better successive interference cancellation (SIC) at the receiver. Finally, sequence grouping based on the cross-correlation properties of sequences is proposed to reduce inter- and intra-group interference. Simulation results show that by incorporating multi-level received powers and sequence grouping into existing NOMA schemes, for an NOMA system with 400% overloading and fixed signature allocation, 3 dB and 10 dB signal-to-noise ratio (SNR) gains at 0.1 block error rate (BLER) target can be achieved compared with existing NOMA schemes and orthogonal multiple access (OMA), respectively. Besides, 0.01 BLER target can be achieved while an error floor exists in existing NOMA schemes. Under random sequence selection, collision probability is reduced by multi-level powers. In addition, GWBE sequences achieve lower BLER than existing sequences and the gain is large especially for low BLER requirements. This shows that the proposed scheme can support larger connectivity and higher reliability.

Key words: Uplink non-orthogonal multiple access; Generalized Welch-bound equality; Multi-level received powers; Sequence grouping

<https://doi.org/10.1631/FITEE.1700842>

CLC number: TN929.5

1 Introduction

With the explosive increase of data rate requirements, mobile communication systems have evolved from the first generation to the fourth generation (4G). In future wireless communication systems (5G and beyond systems), chasing high data rate is no longer the only objective. Based on the recommendation of International Telecommunication Union (ITU) for International Mobile Telecommu-

nication system for 2020 and beyond (IMT-2020), the usage scenarios for 5G and beyond systems include enhanced mobile broadband (eMBB), massive machine-type communications (mMTC), and ultra-reliable and low-latency communications (URLLC) (ITU-R, 2015). With the diversification of usage scenarios and mobile devices, future wireless systems should provide a wider range of services and satisfy requirements such as $1000\times$ average data rate of 4G, 1 ms round-trip latency, and 1 million connections per square kilometer (Andrews et al., 2014; Dahlman et al., 2014; Osseiran et al., 2014).

Non-orthogonal multiple access (NOMA) is

[‡] Corresponding author

 ORCID: Wen-jia LIU, <http://orcid.org/0000-0002-9678-5345>

© Zhejiang University and Springer-Verlag GmbH Germany, part of Springer Nature 2018

a promising technique, which can meet the requirements of various usage scenarios in future wireless communications with specific designs (Dai et al., 2015). Different from orthogonal or pseudo-orthogonal MA (OMA) in existing wireless systems, which can access only a limited number of users to guarantee orthogonality, NOMA can serve multiple users with the same physical (time/frequency) resources with the help of advanced receivers.

NOMA was first proposed for downlink transmission for throughput enhancement (Saito et al., 2013), where users were multiplexed in the power domain. The results showed that power-domain NOMA can achieve $1.5\times$ throughput gain. In Li and Goldsmith (2001) and Tse and Viswanath (2015), both uplink and downlink capacities can be increased by power-domain NOMA and the capacity gain depends on the power difference between users. Therefore, user pairing, power allocation, and scheduling are important for power-domain NOMA and are widely studied (Chen et al., 2014; Ding et al., 2016b). Furthermore, power-domain NOMA can be combined with existing techniques for further performance enhancement (Islam et al., 2017a, 2017b), e.g., cooperative NOMA and multiple-input multiple-output (MIMO)-NOMA. With the specific design of beamforming, user pairing, and power allocation, MIMO-NOMA can achieve a much higher sum rate than OMA-MIMO (Sun et al., 2015; Ding et al., 2016a; Zeng et al., 2017a, 2017b).

To satisfy the requirements of low latency in URLLC, one of the approaches is to omit scheduling or grant from the base station (BS) and users transmit their data blocks in physical resources randomly selected by each user (Nagata et al., 2017; She et al., 2017). Apparently, collisions will occur; i.e., multiple users may transmit signals at the same time and frequency. The existing approach to solve this problem is retransmission or repetition until there is no collision or the data is detected correctly. This will reduce the efficiency of resource utilization. As an enhancement, NOMA can be employed instead of avoiding the collisions for better resource utilization efficiency (Li et al., 2017; Wang et al., 2017).

For mMTC, increasing the connectivity capability is the most challenging target. For the time-division multiple access (TDMA) and the orthogonal frequency-division multiple access (OFDMA), users are allocated orthogonal physical resources. The

total number of users accessing the network simultaneously is limited by the available physical resources. For code-division multiple access (CDMA), users are allocated with long pseudo-random sequences, which are orthogonal asymptotically. However, data blocks in mMTC are usually very small, and long spreading sequences in CDMA are no longer suitable. Various NOMA schemes, such as interleaver-division multiple access (IDMA) (Ping et al., 2006), sparse code multiple access (SCMA) (Nikopour and Baligh, 2013), and multi-user shared access (MUSA) (Yuan et al., 2016), were proposed. These can enhance connectivity capability.

Given the variety of the benefits of NOMA, the 3rd Generation Partnership Project (3GPP) started the standardization of NOMA with Release 13. In Release 13, power-domain NOMA was designed and standardized for downlink transmission and was called downlink multi-user superposition transmission (DL MUST) (3GPP, 2015). In Release 14, NOMA was further studied as a potential technique for new radio (NR). Excepting power, other multiple access (MA) signatures (such as codebook, sequences, interleaver, and mapping pattern) were employed to distinguish multiple users and facilitated multi-user detection (MUD) at the receiver. Comprehensive link-level and system-level evaluation results showed that NOMA has significant gain in terms of uplink throughput and overloading capability over OMA (3GPP, 2017b).

Due to limited time, the study of NOMA in Release 14 stopped before completion. Therefore, study item for NOMA was continued in Release 15, which focused on uplink and targeted to provide recommendation on the NOMA scheme(s) to be specified later. To this end, comprehensive evaluations are necessary and potential enhanced and hybrid designs are important for a recommendation.

Power as one of MA signatures has been employed for DL MUST in Release 13 and power-domain NOMA has been widely investigated in academia. However, NOMA in Releases 14 and 15 usually assumes equal received power and power has not so far been fully exploited. Considering the near-far effect, power difference is a natural phenomenon in wireless networks. How to employ the feature of power difference to further enhance the performance of uplink NOMA is an important issue.

As an important category of NOMA schemes,

sequence-based NOMA schemes employ user-specific sequences as MA signatures and can obtain good trade-off between performance and complexity. NOMA schemes using user-specific sequences as the MA signature are defined as sequence-based NOMA schemes in this study. However, existing sequence-based NOMA schemes cannot support high connectivity either because of the limited number of sequences or because of poor performance of cross-correlations. How to use these existing sequences to support high connectivity should be further studied.

We first propose power as part of MA signatures to increase connectivity capability and reliability of uplink NOMA. Based on the unequal received powers of multiple users, we propose a new kind of spreading sequences, and two schemes that can be combined with existing sequence-based NOMA schemes for performance enhancement. The evaluation results based on link-level simulations show that the proposed schemes and sequences can enhance performance compared with existing sequence-based NOMA schemes. The contributions of this paper are summarized as follows:

1. We first propose to use sequences targeting at generalized Welch-bound equality (GWBE) as spreading sequences in NOMA. This will maximize the ergodic capacity for systems with unequal received powers.
2. We propose user grouping with multi-level received powers to facilitate MUD at the receiver, where users in one group have equal received power while users in different groups have different received powers.
3. We investigate the sequence grouping based on the property of cross-correlations to reduce inter- and intra-group interference. Two algorithms for sequence grouping are proposed for different power offsets between adjacent groups.

2 Introduction of non-orthogonal multiple access (NOMA) study

2.1 NOMA schemes for standardization in 3GPP

NOMA was first proposed to increase the system capacity for downlink systems, known as DL MUST in Release 13 (3GPP, 2015). In DL MUST, the BS transmits a superposed signal for multiple users with

different transmit powers with the same physical resources. Successive interference cancellation (SIC) is applied at the receivers to mitigate the inter-user interference.

With the diversification of requirements in future wireless communications, NOMA is also designed for uplink transmission to provide the capability of massive connectivity and low latency. For NOMA in Releases 14 and 15, schemes have been proposed as listed in Table 1. Different from using power as the only approach to distinguish users in DL MUST, various signatures, such as bit-level interleaver/scrambler, multi-dimensional constellation, symbol-level interleaver/scrambler, symbol-level spreading sequences, and symbol-to-resource element (RE) mapping pattern at the transmitter, are exploited by NOMA schemes. With the help of advanced receivers, signals of multiple users can be detected successfully.

2.1.1 Unified structure at the transmitter

Even though various signatures are employed by different NOMA schemes, the principle of trying to distinguish users at the receiver by different MA signatures is a common feature. Therefore, the transmitter of NOMA schemes can be unified into one common structure consisting of six modules as shown in Fig. 1.

1. Bit-level interleaver/scrambler

For NOMA schemes with bit-level operations, user-specific bit-level interleaver/scrambler combined with low code rate channel coding is used to help MUD at the receiver (Ping et al., 2006).

2. Bit-to-symbol mapping

This module maps the coded bits into modulated symbols, where no user-specific design is considered. For NOMA schemes other than SCMA, conventional modulation schemes (e.g., binary phase shift keying and quadrature phase shift keying) are used. To further exploit the gain of this module, multi-dimensional modulation with shaping gain is used in SCMA (Taherzadeh et al., 2014).

3. Symbol stream generation

Most NOMA schemes with symbol-level operations provide user-specific designs in this module, such as symbol-level interleaver and/or scrambler, and user-specific spreading sequences (Table 1).

4. Power adjustment

Power is a simple but effective approach to

Table 1 Existing non-orthogonal multiple access (NOMA) schemes ordered by date

Scheme	Feature	Reference
SCMA	Multi-dimensional constellation and sparse symbol-to-RE mapping pattern	3GPP (2016a)
RSMA	Symbol-level scrambler	3GPP (2016b)
MUSA	Random complex spreading sequences	3GPP (2016c)
PDMA	Symbol-to-RE mapping pattern	3GPP (2016d)
LCRS	Low code rate and bit-level interleaver	3GPP (2016e)
NCMA	Grassmannian spreading sequences	3GPP (2016f)
IGMA	Bit-level interleaver and symbol-level grid mapping pattern	3GPP (2016g)
LDS-SVE	Signature vector extension and RB-based sparse mapping pattern	3GPP (2016h)
LSSA	Low code rate, user-specific bit-level permutation pattern, and group RS pattern	3GPP (2016i)
NOCA	Long term evolution (LTE) defined sequences for uplink RS	3GPP (2016j)
IDMA	Low code rate and bit-level interleaver	3GPP (2016k)
SSMA	Short spreading sequences	3GPP (2016l)
NOMA	Orthogonal spreading sequences	3GPP (2016n)
RDMA	Cyclic-shift repetition and symbol-level interleaver	3GPP (2016o)
GOCA	Orthogonal sequences in one group and non-orthogonal sequences for different groups	3GPP (2016o)

distinguish users. Most NOMA schemes assume equal power, i.e., no power adjustment among users, except power-domain NOMA, which employs user-specific power.

5. Symbol-to-RE mapping

The symbols can be mapped into either all the available physical resources (i.e., full mapping) or part of available physical resources (i.e., sparse mapping). Sparse mapping can reduce the collision on each RE at the cost of less transmission resource and user-specific mapping patterns can be designed to facilitate MUD (Chen et al., 2017). Full mapping can fully use the resources at the cost of more interference.

From the features indicated in Table 1, one or multiple user-specific modules in Fig. 1 are used by each NOMA scheme as its MA signature to help receivers distinguish users and the left modules are cell-specific or identical for all users. For example, MUSA and power-domain NOMA use the module of symbol stream generation with user-specific sequences and the module of power adjustment with user-specific powers, respectively; i.e., only one user-specific module is employed. In contrast, IGMA uses two user-specific modules, i.e., interleaver/scrambler with user-specific bit-level interleaver and symbol stream generation with user-specific symbol-level interleaver, as MA signatures.

2.1.2 Advanced receiver

Besides MA signatures at the transmitter, another common feature of NOMA schemes is to allow MUD at the receiver (3GPP, 2017b). In the study

item of NOMA in Release 14, MUD is also widely discussed for various NOMA schemes.

1. Message passing algorithm (MPA) receiver

As one kind of maximum likelihood (ML) receiver, the MPA receiver can achieve approximately optimal performance (Wu et al., 2015). However, the complexity increases exponentially with the maximum number of users superposed at the same RE. This is very high for an NOMA system with high overloading. Given high complexity, MPA is more suitable for NOMA schemes with sparse symbol-to-RE mapping, such as SCMA, PDMA, and IGMA.

2. Elementary signal estimator (ESE) receiver

ESE is a soft-cancellation based receiver (Ping et al., 2006), which is mostly used by NOMA schemes with bit-level operations such as IDMA, LCRS, and IGMA. The complexity increases linearly with the number of users.

3. SIC receiver

Power differences among multiple users at the receiver are exploited by the SIC receiver, where users are detected and canceled from the received signals successively in the order of received power (Endo et al., 2012). The complexity increases linearly with the number of users with the same physical resources. The SIC receiver can be applied by all NOMA schemes. In addition, SIC can be combined with MPA and ESE for complexity reduction or performance enhancement.

Based on the NOMA schemes (Table 1) and the unified structure (Fig. 1), we find that the module of symbol stream generation is mostly exploited for user-specific design in existing NOMA schemes.

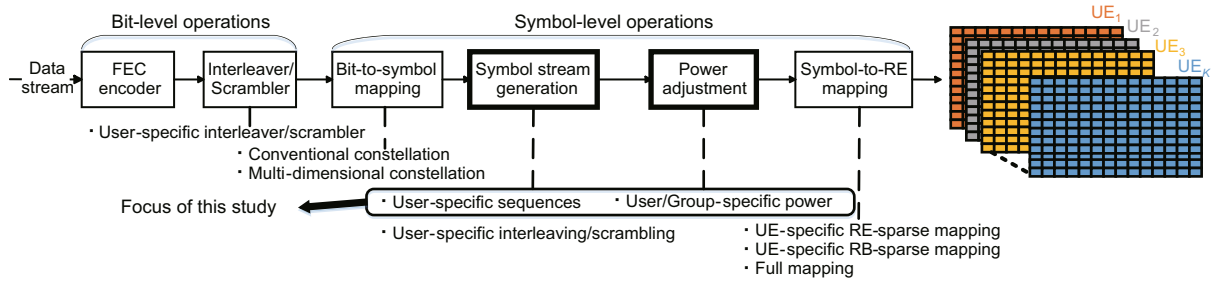


Fig. 1 Unified structure of non-orthogonal multiple access schemes at the transmitter

Among all the approaches for symbol stream generation, user-specific spreading sequences are most popular. On the one hand, evaluation results based on link-level simulations and system-level simulations in 3GPP (2017b) show that sequence-based NOMA schemes can achieve good performance on both connectivity capability and reliability. On the other hand, the complexity of sequence-based NOMA schemes is low because of low complexity at the SIC receiver. Therefore, sequence-based NOMA schemes can achieve good trade-off between performance and complexity and are the focus of this study.

2.2 Sequence-based NOMA schemes

Sequence-based NOMA schemes are a large family including MUSA, SSMA, NCMA, NOCA, NOMA, and GOCA, which all use symbol stream generation with user-specific sequences at the transmitter (Fig. 1) and SIC at the receiver. The only difference among these schemes is the sequences in symbol stream generation. In this subsection, sequences used in existing sequence-based NOMA schemes are introduced.

2.2.1 Sequences in existing NOMA schemes

Consider an uplink NOMA system, where K single-antenna users are multiplexed with the same physical resources. To simplify notations, single-antenna BS is assumed. The results can be easily extended to multi-antenna BSs. The modulated symbols of the k^{th} user (denoted as UE_k) are spread by a user-specific sequence $\mathbf{s}_k \in \mathbb{C}^{N \times 1}$ with N being the spreading factor. Assuming an additive white Gaussian noise (AWGN) channel, the received signal at the BS is

$$\mathbf{y} = \sum_{k=1}^K \sqrt{P_k} \mathbf{s}_k x_k + \mathbf{n}, \quad (1)$$

where P_k is the received power of UE_k , $\|\mathbf{s}_k\| = 1$, x_k is the modulated symbol, $\mathbf{n} \sim \mathcal{CN}(\mathbf{0}, \sigma^2 \mathbf{I}_N)$ is the AWGN noise at the receiver, σ^2 denotes the noise variance, \mathbf{I}_N denotes the identity matrix with dimension N , and $\mathcal{CN}(\mathbf{m}, \mathbf{\Sigma})$ denotes a complex Gaussian distribution with mean \mathbf{m} and covariance $\mathbf{\Sigma}$.

As the MA signature in sequence-based NOMA schemes, sequences are the key factor in determining the performance. The sequences for all users are selected by each user or allocated by the BS from the sequence pool $\mathcal{S} = [\mathbf{s}_1, \mathbf{s}_2, \dots, \mathbf{s}_L]$ with L sequences. In existing NOMA schemes, sequences in \mathcal{S} are designed either under the assumption of equal received power or without considering the effects of power. Therefore, in this subsection, equal received power for multiple users, i.e., $P_k = P, \forall k$, is assumed.

1. Welch-bound equality (WBE) sequences

For equal received power, the optimal sequences maximizing ergodic sum capacity can be obtained by

$$\max_{\mathbf{S}: \mathbf{s}_k^H \mathbf{s}_k = 1 \forall k} C_{\text{sum}} = \frac{1}{2N} \log_2 \left(\det \left(\mathbf{I}_N + \frac{P}{\sigma^2} \mathbf{S} \mathbf{S}^H \right) \right), \quad (2)$$

where $\mathbf{S} = [\mathbf{s}_1, \mathbf{s}_2, \dots, \mathbf{s}_K] \in \mathbb{C}^{N \times K}$ and $(\cdot)^H$ denotes the conjugate transpose of a matrix.

For non-overloaded systems, i.e., $K \leq N$, it is easy to verify that orthogonal sequences are optimal and the sum capacity is $C_{\text{sum}} = \frac{K}{2N} \log_2 \left(1 + \frac{P}{\sigma^2} \right)$. Henceforth, we assume $K > N$, i.e., overloaded systems in the sequel.

Based on Massey and Mittelholzer (1993), Viswanath and Anantharam (1999), and Datta et al. (2012), sequences that meet equality in Welch-bound (known as WBE sequences) are capacity optimal for equal received power. The Welch-bound was first proposed in Welch (1974), and was defined as the lower-bound of the total l -squared correlation (TSC)

of sequences with unit power:

$$T_{\text{SC}} = \sum_{i=1}^K \sum_{j=1}^K |s_i^H s_j|^2 \geq \frac{K^2}{\binom{N+l-1}{l}}, \quad (3)$$

where $l \geq 1$ and $\binom{n}{k}$ denotes the number of k -combinations from a set with n elements. For the special case with $l = 1$, Welch-bound in inequality (3) becomes $T_{\text{SC}} \geq \frac{K^2}{N}$ and WBE sequences in \mathbf{S} satisfy $\mathbf{S}\mathbf{S}^H = \frac{K}{N}\mathbf{I}_N$, which can be obtained by algorithms in Dhillon et al. (2005).

By substituting $K = L$ into Eq. (2) and inequality (3), WBE sequence pool $\mathcal{S} = \mathbf{S}$ can be obtained for any pool size L .

2. Grassmannian sequences

Grassmannian sequences are employed as user-specific sequences in NCMA (3GPP, 2016f) and aim at maximizing the minimum chordal distance between codeword pairs:

$$\min_{\mathbf{S}: s_k^H s_k = 1 \forall k} \left(\max_{1 \leq k < j \leq K} \sqrt{1 - |s_k^H s_j|^2} \right). \quad (4)$$

The optimal solution of Eq. (4) satisfies $|s_i^H s_j| = \sqrt{1 - \frac{(N-1)K}{N(K-1)}} \forall i \neq j$; i.e., the cross-correlation for any two different sequences is constant and can be obtained by algorithms in Medra and Davidson (2014).

It is easy to verify that Grassmannian sequences achieve the lower-bound in inequality (3) and are one kind of WBE sequences. This indicates that Grassmannian sequences are capacity optimal. Similar to WBE sequences, the sequence pool with any size L can be obtained by substituting $K = L$ into Eq. (4).

However, the elements in both Grassmannian and WBE sequences are irregular complex values, which may increase the complexity for hardware implementation. To avoid this problem, the following sequences are also proposed for NOMA.

3. Constant amplitude zero autocorrelation (CAZAC) sequences

CAZAC sequences are usually used as uplink reference signal (RS) sequences in long term evolution (LTE) (3GPP, 2012). For sequence length $N = 6, 12, 18, 24$, computer generated CAZAC sequences can be given as

$$s_u^{(\alpha)}(n) = \exp(j\alpha n) \exp\left(j \frac{\varphi(n)\pi}{4}\right), \quad 0 \leq n < N, \quad (5)$$

where α is the cyclic shift (CS) and $\varphi(n)$ is given in 3GPP (2012). $s_u^{(\alpha)} = [s_u^{(\alpha)}(0), s_u^{(\alpha)}(1), \dots, s_u^{(\alpha)}(N-1)]^T$ is the spreading sequence with CS α and root u . Sequences with one root and different CSs are orthogonal, while sequences with different roots are non-orthogonal. For $N = 12$, there are 30 available roots and 12 available CSs for each root. In this case, the sequence pool is $\mathcal{S} = [s_u^{(2\pi \cdot v/12)}]$ for $u = 0, 1, \dots, 29$ and $v = 0, 1, \dots, 11$ with pool size $L = 360$.

CAZAC sequences in Eq. (5) are employed as spreading sequences in NOCA (3GPP, 2016j) and can provide good properties such as constant modulus and thus low cubic metric and good autocorrelation. However, the length of CAZAC sequences in Eq. (5) is limited to $\{6, 12, 18, 24\}$, which reduces the flexibility.

4. Orthogonal variable spreading factor (OVSF) sequences

OVSF sequences belong to orthogonal sequences and are used as user-specific sequences in NOMA (3GPP, 2016n). The length of OVSF sequences N could only be a power of 2, i.e., $N = 2^n \forall n \in \mathbb{N}_+$. For $N = 2^n$, OVSF sequences can be obtained recursively as

$$\mathbf{S}^{(n)} = \begin{bmatrix} \mathbf{S}^{(n-1)} & \mathbf{S}^{(n-1)} \\ \mathbf{S}^{(n-1)} & -\mathbf{S}^{(n-1)} \end{bmatrix}, \quad (6)$$

where $\mathbf{S}^{(0)} = 1$ and $\mathbf{S} = \mathbf{S}^{(n)}/\sqrt{N}$ with $L = N$.

The elements of OVSF sequences are either 1 or -1 . This is beneficial for hardware implementation. The pool size of OVSF sequences is equal to the sequence length, which is N here. Because of the small number of sequences, the complexity of blind detection is low. However, orthogonal sequences cannot enhance the connectivity but only improve the receiver performance (3GPP, 2016n).

5. Random complex sequences

Random complex sequences were proposed by Yuan et al. (2016) and used as spreading sequences in MUSA (3GPP, 2016c). Different from OVSF sequences, the sequences for MUSA are complex and the values of real and imaginary parts are chosen from $\{-1, 1\}$. Therefore, each element of the complex spreading sequences is from the set $\{1 + i, 1 - i, -1 + i, -1 - i\}$ before normalization and the number of available sequences is $L = 4^N$.

To further increase the number of available sequences, the value sets of real and imaginary parts

could expand to $\{-1, 0, 1\}$. In this case, each element of the complex spreading sequences is from the set $\{1+i, -1+i, i, 1, -1, 0, 1-i, -1-i, -i\}$ before normalization. Since each element can be chosen from 9 values, $L = 9^N - 1$ sequences with non-zero norm could be generated. Based on 3GPP (2017a), part of the sequences with low cross-correlations can be further selected from the original pool with $L = 4^N$ or $L = 9^N - 1$ sequences to form a new sequence pool with smaller pool size but lower cross-correlation.

2.2.2 Power in existing NOMA schemes

Besides sequences, power is a simple but effective signature for performance enhancement.

1. NOMA schemes based on equal received power

Existing NOMA schemes usually assume equal average received power by accurate uplink power control based on the path loss. From Section 2.2.1, we know that all sequence designs consider no power differences.

However, as a natural phenomenon, a near-far effect exists in cellular networks. As shown in DL MUST, power difference can further enhance the performance with the help of an SIC receiver.

2. NOMA schemes based on unequal transmit power

As an enhancement of NCMA, demodulation RS (DMRS)-staggered NCMA was proposed in 3GPP (2016m), where group-specific transmit power offsets are used to facilitate SIC receiving and the same spreading sequences are reused in multiple groups. On the one hand, the performance of the SIC receiver depends on the received power instead of transmit power. On the other hand, reusing the same spreading sequences leads to soft collision among users in different groups, which may lead to poor performance.

3. NOMA schemes based on unequal received power

Zadoff-Chu (ZC) sequence design with power-based grouping scheme was proposed in Teng et al. (2017), where ZC sequences with one root and different cyclic shifts were used in one group. ZC sequences with different roots were used in different groups. On the one hand, the length of ZC sequences is selected from set $\{6, 12, 18, 24, \dots\}$, which belongs to

long spreading sequences and the performance is limited by poor channel estimation accuracy and error propagation of the SIC (3GPP, 2017a). On the other hand, the number of sequences in one group is limited to the largest number of cyclic shifts to maintain orthogonality, which reduces the flexibility.

To further enhance performance, in the next section, multi-level average received powers are proposed as part of the MA signature; i.e., two modules of symbol stream generation with user-specific sequences and power adjustment with group-specific powers in Fig. 1 are employed as the MA signature. The impact of multi-level average received powers is discussed from the perspective of a new design of the sequence pool and flexible usage of existing and new sequence pools, respectively.

3 Proposed non-orthogonal multiple access (NOMA) enhancements

In this section, three enhancements for uplink NOMA are proposed. We first design the capacity optimal sequences under unequal received power and then propose user grouping with multi-level received powers and sequence grouping to facilitate SIC receiving and enhance performance.

3.1 Capacity optimal sequence design under unequal received power

Under unequal received power, WBE sequences in Eq. (2) are no longer capacity optimal and the problem of maximizing ergodic sum capacity becomes

$$\begin{aligned} \max_{\mathbf{S}: \mathbf{s}_k^H \mathbf{s}_k = 1 \forall k} C_{\text{sum}} &= \frac{1}{2N} \log_2 \left(\det \left(\mathbf{I} + \frac{1}{\sigma^2} \mathbf{S} \mathbf{P} \mathbf{S}^H \right) \right) \\ &= \frac{1}{2N} \sum_{n=1}^N \log_2 \left(1 + \frac{1}{\sigma^2} \lambda_n \right), \end{aligned} \quad (7)$$

where $\mathbf{P} = \text{diag}(P_1, P_2, \dots, P_K)$ is a diagonal matrix whose diagonal elements are the received powers of all the K users and λ_n is the n^{th} eigenvalue of matrix $\mathbf{S} \mathbf{P} \mathbf{S}^H$. This indicates that the sum capacity is determined by $\mathbf{S} \mathbf{P} \mathbf{S}^H$ instead of $\mathbf{S} \mathbf{S}^H$ for unequal received powers.

Define that UE $_k$ is oversized if

$$P_k > \frac{\sum_{i=1}^K P_i \cdot \text{sign}(P_i > P_k)}{N - \sum_{i=1}^K \text{sign}(P_i \geq P_k)}, \quad (8)$$

where $\text{sign}(x)$ equals 1 or 0 if condition x is true or false, respectively. Therefore, a user is oversized if its received power is large relative to the received powers of other users.

Denote the set of oversized users as \mathcal{K} . Based on the analysis in Viswanath and Anantharam (1999) and Viswanath et al. (1999), under the given received power \mathbf{P} , the optimal eigenvalues $\boldsymbol{\lambda}^* = [\lambda_1^*, \lambda_2^*, \dots, \lambda_N^*]$ of $\mathbf{S}^* \mathbf{P} (\mathbf{S}^*)^H$ can be derived as

$$\boldsymbol{\lambda}^* = \left[\underbrace{\frac{\sum_{i \notin \mathcal{K}} P_i}{N - |\mathcal{K}|}, \dots, \frac{\sum_{i \notin \mathcal{K}} P_i}{N - |\mathcal{K}|}}_{N - |\mathcal{K}| \text{ elements}}, \underbrace{P_j}_{|\mathcal{K}| \text{ elements}}; j \in \mathcal{K} \right], \quad (9)$$

where $|\mathcal{K}|$ denotes the number of oversized users. The maximum sum capacity can be easily obtained as $C_{\text{sum}} = \frac{N - |\mathcal{K}|}{2N} \log_2 \left(1 + \frac{\sum_{i \notin \mathcal{K}} P_i}{(N - |\mathcal{K}|)\sigma^2} \right) + \frac{1}{2N} \sum_{j \in \mathcal{K}} \log_2 \left(1 + \frac{P_j}{\sigma^2} \right)$. The optimal sequences \mathbf{S}^* can then be obtained based on Eq. (9) as follows.

For oversized users $i \in \mathcal{K}$, let $\mathbf{s}_i = [0, \dots, 0, 1, 0, \dots, 0]^T$ with entry 1 in the i^{th} position. We can then construct sequences for the remaining $(K - |\mathcal{K}|)$ non-oversized users from the orthogonal space of oversized users, which has $(N - |\mathcal{K}|)$ dimensions (Viswanath et al., 1999). Based on the algorithms in Dhillon et al. (2005) for constructing Hermitian matrices with prescribed diagonal entries and eigenvalues, the optimal sequences for non-oversized users can be obtained. The detailed algorithm constructing optimal sequences \mathbf{S}^* for given received power \mathbf{P} is provided in Algorithm 1.

When $\sum_{k=1}^K P_k \geq N \cdot \max\{P_1, P_2, \dots, P_K\}$, the powers of multiple users are close enough and there are no oversized users; i.e., $\mathcal{K} = \phi$. In this case, Eq. (9) reduces to $\boldsymbol{\lambda}^* = \frac{\sum_i P_i}{N} \mathbf{1}_N$ and the optimal sequences satisfy $\mathbf{S}^* \mathbf{P} (\mathbf{S}^*)^H = \frac{\sum_i P_i}{N} \mathbf{I}_N$, which are called generalized WBE (GWBE) sequences. It can be easily found that when $P_k = P$ for $\forall k$, $\mathbf{P} = P \mathbf{I}_K$ and the optimal sequences satisfy $\mathbf{S}^* (\mathbf{S}^*)^H = \frac{K}{N} \mathbf{I}_N$, which reduces to WBE sequences. This indicates that Algorithm 1 can be used for constructing both GWBE and WBE sequences.

Similar to TSC under equal received power in inequality (3), the weighted TSC under unequal received power is lower-bounded by

$$T_{\text{SC}} = \sum_{i=1}^K \sum_{j=1}^K P_i P_j |\mathbf{s}_i^H \mathbf{s}_j|^2 \geq \frac{\left(\sum_{k=1}^K P_k \right)^2}{N}, \quad (10)$$

Algorithm 1 Construction of optimal sequences

- 1: Find the set of oversized users \mathcal{K} satisfying $P_k > \frac{\sum_{i=1}^K P_i \cdot \text{sign}(P_i > P_k)}{N - \sum_{i=1}^K \text{sign}(P_i \geq P_k)}$ for $k \in \mathcal{K}$.
 - 2: Construct a matrix $\mathbf{Q} \in \mathbb{C}^{(K - |\mathcal{K}|) \times (K - |\mathcal{K}|)}$ with diagonal elements $\{P_i \mid i \notin \mathcal{K}\}$ and eigenvalues $\left[\frac{\sum_{i \notin \mathcal{K}} P_i}{N - |\mathcal{K}|} \mathbf{1}_{N - |\mathcal{K}|}^T, \mathbf{0}_{(K - N) \times 1}^T \right]^T$ with ‘generalized Chan-Li’ or ‘generalized Bendel-Mickey’ algorithms in Dhillon et al. (2005).
 - 3: Decompose $\mathbf{Q} = \mathbf{U} \boldsymbol{\Lambda} \mathbf{U}^H$, where \mathbf{U} is the matrix of eigenvectors.
 - 4: Denote the eigenvectors in \mathbf{U} corresponding to the non-zero eigenvalues as $\check{\mathbf{U}} \in \mathbb{C}^{(N - |\mathcal{K}|) \times (N - |\mathcal{K}|)}$ and the non-zero eigenvalues as $\check{\boldsymbol{\Lambda}} = \frac{\sum_{i \notin \mathcal{K}} P_i}{N - |\mathcal{K}|} \mathbf{I}_{N - |\mathcal{K}|}$.
 - 5: Construct sequences $\check{\mathbf{S}} = \check{\boldsymbol{\Lambda}}^{\frac{1}{2}} \check{\mathbf{U}}^H \check{\mathbf{P}}^{-\frac{1}{2}}$, where $\check{\mathbf{P}} = \text{diag}\{P_i \mid i \notin \mathcal{K}\}$.
// Construct sequences to non-oversized users
 - 6: Construct $\mathbf{S} = \mathbf{C}_{\text{orth}} \begin{bmatrix} \mathbf{I}_{|\mathcal{K}|} & \mathbf{0}_{|\mathcal{K}| \times (K - |\mathcal{K}|)} \\ \mathbf{0}_{(N - |\mathcal{K}|) \times |\mathcal{K}|} & \check{\mathbf{S}} \end{bmatrix}$,
where $\mathbf{C}_{\text{orth}} \in \mathbb{C}^{N \times N}$ is any orthogonal matrix satisfying $\mathbf{C}_{\text{orth}} \mathbf{C}_{\text{orth}}^H = \mathbf{I}_N$.
// Construct sequences of all users
-

where the equality could be achieved by GWBE sequences.

For an NOMA scheme with GWBE sequences, the average received powers $\{P_1, P_2, \dots, P_K\}$ should be first defined and then the corresponding GWBE sequences $\{\mathbf{s}_1, \mathbf{s}_2, \dots, \mathbf{s}_K\}$ are generated by Algorithm 1 for $\{P_1, P_2, \dots, P_K\}$. In this case, a set of power and sequence $\{P_k, \mathbf{s}_k\}$ is used as an MA signature.

As described in Section 2.1.2, SIC is commonly used by sequence-based NOMA schemes. Assuming an SIC receiver without error propagation in a coded system (Guess and Varanasi, 2000), the signal-to-interference-plus-noise ratio (SINR) of UE $_k$ under matched filter (MF) is

$$\gamma_k = \frac{P_k}{\sum_{\{j|P_j \leq P_k\}} |\mathbf{s}_k^H \mathbf{s}_j|^2 + \sigma^2}, \quad (11)$$

where $\{j|P_j \leq P_k\}$ denotes the index set of users with lower received power than UE $_k$.

It can be easily found that with an SIC receiver, power difference among users at the receiver is very important. However, existing NOMA schemes either assume equal received power or group users based on the transmit power instead of received powers as shown in Section 2.2. In addition, Eq. (11) indicates

that the performance is affected by cross-correlation of sequences used by users with lower received power instead of all users, while all sequence designs in existing NOMA schemes in Section 2.2.1 focus on the cross-correlations of all sequences instead of sequences of users with lower received powers.

We discuss a new design of sequences for unequal powers, i.e., GWBE sequences. To further exploit and use power in existing NOMA schemes, a combination of power and existing sequences is proposed as MA signatures and discussed. To this end, user grouping with multi-level received powers and sequence grouping are proposed to reduce inter- and intra-group multi-user interference (MUI) for performance enhancement in the following.

3.2 User grouping with multi-level received powers

To facilitate SIC receiving, K users are divided into G groups, where users in one group have equal received power and received powers of users in multiple groups are different. Denote \mathcal{K}_g , $K_g = |\mathcal{K}_g|$, and \tilde{P}_g as the set of user indices, number of users, and received power in the g^{th} group, respectively. Without loss of generality, we assume $\tilde{P}_1 \geq \tilde{P}_2 \geq \dots \geq \tilde{P}_G$ as shown in Fig. 2. The total power remains constant; i.e., the average received power remains $\frac{1}{K} \sum_{k=1}^K P_i = \frac{1}{K} \sum_{g=1}^G K_g \tilde{P}_g = P$. Note that when $\tilde{P}_1 = \tilde{P}_2 = \dots = \tilde{P}_G$, NOMA with user grouping reduces to existing NOMA schemes.

With the multi-level received powers, the SINR of UE $_k$ in the g^{th} group becomes

$$\gamma_k = \left(\underbrace{\sum_{j \in \mathcal{K}_g \setminus \{k\}} |\mathbf{s}_k^H \mathbf{s}_j|^2}_{\text{MUI of users in one group}} + \underbrace{\sum_{m=g+1}^G \sum_{j \in \mathcal{K}_m} \frac{\tilde{P}_m}{\tilde{P}_g} |\mathbf{s}_k^H \mathbf{s}_j|^2}_{\text{MUI of users in groups with lower power}} + \frac{\sigma^2}{\tilde{P}_g} \right)^{-1}, \quad (12)$$

where $\mathcal{K}_g \setminus \{k\}$ denotes the index set of users in group g except UE $_k$.

Comparing Eqs. (11) and (12), we find that through multi-level received powers, $\frac{\tilde{P}_m}{\tilde{P}_g} < 1$ can be set to a certain value to facilitate SIC and the performance is then improved.

3.3 Sequence grouping

From Eq. (12), we find that the impacts of sequences on the SINR depend on the received powers and are different. For example, the SINR of UE $_k$ in

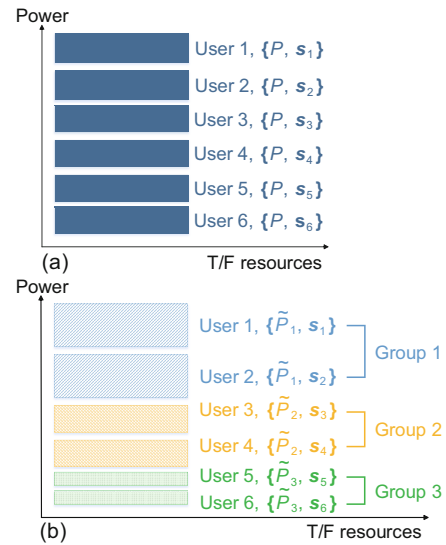


Fig. 2 Illustration of non-orthogonal multiple access (NOMA) with six users ($K = 6$): (a) NOMA with equal received power; (b) NOMA with user grouping and multi-level received powers ($G = 3$, $K_1 = K_2 = K_3 = 2$, and $\tilde{P}_1 > \tilde{P}_2 > \tilde{P}_3$)

group g is determined by the cross-correlations between \mathbf{s}_k and sequence subsets $\{\mathbf{s}_j \mid j \in \mathcal{K}_g \setminus \{k\}\}$ and $\{\mathbf{s}_j \mid j \in \mathcal{K}_m\}$ for $m = \{g+1, g+2, \dots, G\}$ in decreasing order of impact. This indicates that sequences can be divided into multiple groups based on the cross-correlations and SIC orders for further performance enhancement.

For any sequence pool $\mathcal{S} \in \mathbb{C}^{N \times L}$ with L unit-power sequences (e.g., all existing sequence pools in Section 2.2.1 and the new sequence pool in Section 3.1 can be used), the L sequences in the pool are divided into G groups $\{\mathcal{S}_1, \mathcal{S}_2, \dots, \mathcal{S}_G\}$, where $\mathcal{S}_g \in \mathbb{C}^{N \times L_g}$ with L_g sequences are allocated for group g .

Remark 1 For the proposed NOMA scheme with user grouping, the MA signature is extended from a user-specific sequence \mathbf{s} to a set $\{\tilde{P}, \mathbf{s}\}$. Therefore, the total number of MA signatures becomes $\sum_{g=1}^G L_g$, which can be smaller than, equal to, or larger than L based on the connectivity requirement. For example, for the scenario with the large connectivity requirement $K \geq GL$, increasing the number of MA signatures is very important and $\sum_{g=1}^G L_g$ should be as large as possible. In this case, the sequence pool can be reused for all the G groups, i.e., $L_g = L$. While for the scenario with medium to low requirements $K \leq L$, reducing cross-correlations among sequences in one or multiple groups is more

important. In this case, the L sequences should be divided into G groups without collision.

Without loss of generality, we assume $\sum_{g=1}^G L_g = L$ in what follows. Based on the analysis in Section 3.1, we know that the optimal sequences in group g should satisfy

$$\min_{\mathbf{S}_g} \sum_{m,n \geq g} \sum_{i \in \mathcal{K}_m} \sum_{j \in \mathcal{K}_n} \tilde{P}_m \tilde{P}_n |\mathbf{s}_i^H \mathbf{s}_j|^2. \quad (13)$$

The weighted TSC of sequences in group g and groups with smaller received power than group g should be minimized. From Eq. (10), we know that the sequences targeting to $(\sum_{m=g}^G K_m \tilde{P}_m)^2 / N$ minimize Eq. (13) and are optimal for group g .

Considering the complexity of implementation and large storage requirement of optimal sequence grouping for any multi-level received power, we focus on two extreme cases in the following.

3.3.1 Large power offset

When the power offset between adjacent groups is large enough ($\tilde{P}_m / \tilde{P}_g \ll 1$), the interference caused by users with lower received power can be neglected. The SINR in Eq. (12) can be approximated by

$$\gamma_k \approx \left(\sum_{j \in \mathcal{K}_g \setminus \{k\}} |\mathbf{s}_k^H \mathbf{s}_j|^2 + \frac{\sigma^2}{\tilde{P}_g} \right)^{-1}. \quad (14)$$

It is clear that the performance depends on the cross-correlations of sequences in one group, while the cross-correlations of sequences in different groups have nearly no impact on performance. In this case, the sequences with low-correlations should be allocated into one group and problem (13) reduces to

$$\min_{\mathbf{S}_g} \sum_{i,j \in \mathcal{K}_g} |\mathbf{s}_i^H \mathbf{s}_j|^2, \quad (15)$$

which indicates that sequences targeting to Welch-bound equality in Eq. (10) should be selected into one group. Further considering the priority of G groups in SIC receiving, sequences for groups with higher received power should be first selected from the pool. The details are given in Algorithm 2.

3.3.2 Small power offset

When the power offset between adjacent groups is small, i.e., $\tilde{P}_m / \tilde{P}_g \approx 1$, the interference caused by users with lower received power cannot be neglected.

Algorithm 2 Sequence grouping for large power offset

- 1: Let $g = 1$ and $\mathbf{S}^{(1)} = \mathbf{S}$. // Initialization
 - 2: **loop**
 - 3: **if** $g < G$ **then**
 - 4: Find all $A = \binom{L - \sum_{m=1}^{g-1} L_m}{L_g}$ combinations of L_g sequences from sequence pool $\mathbf{S}^{(g)}$. Denote L_g sequences in the a^{th} combination as $\mathbf{S}_a^{(g)}$.
 - 5: Find the optimal combination index a^* for group g satisfying

$$\min_{1 \leq a \leq A} \sum_{\mathbf{s}_i, \mathbf{s}_j \in \mathbf{S}_a^{(g)}} |\mathbf{s}_i^H \mathbf{s}_j|^2.$$
 - 6: The sequences for group g are $\mathbf{S}_g = \mathbf{S}_{a^*}^{(g)}$.
 - 7: Update $g = g + 1$ and $\mathbf{S}^{(g)} = \mathbf{S}^{(g-1)} \setminus \mathbf{S}_{g-1}$, where $\mathbf{S}^{(g-1)} \setminus \mathbf{S}_{g-1}$ denotes the sequences in $\mathbf{S}^{(g-1)}$ except \mathbf{S}_{g-1} .
 - 8: **end if**
 - 9: **end loop**
-

The SINR in Eq. (12) can be approximated by

$$\gamma_k \approx \left(\sum_{m=g}^G \sum_{j \in \mathcal{S}_m} |\mathbf{s}_k^H \mathbf{s}_j|^2 - |\mathbf{s}_k^H \mathbf{s}_k|^2 + \frac{\sigma^2}{\tilde{P}_g} \right)^{-1}. \quad (16)$$

In this case, not only the cross-correlations of sequences in the same group matter, but also the cross-correlations of sequences in groups with lower received powers are important. The user with higher SIC order, i.e., larger received power, will suffer MUI from more users. To reduce MUI, sequences with lower total cross-correlations are allocated to groups with higher received power. For group g , the sequences should satisfy

$$\min_{\mathbf{S}_g} \sum_{i \in \{\mathcal{K}_m | m \geq g\}} \sum_{j \in \{\mathcal{K}_n | n \geq g\}} |\mathbf{s}_i^H \mathbf{s}_j|^2, \quad (17)$$

where $\{\mathcal{K}_m | m \geq g\}$ denotes the index set of users in groups with the same and smaller received power than group g . The details are shown in Algorithm 3.

3.3.3 Examples for sequence grouping

To make the algorithms clearer, examples for sequence grouping under large and small power offsets are provided in this subsection. Random complex sequences in Eq. (18) are used as spreading sequences of the NOMA system with $K = 6$ users and spreading factor $N = 4$. The pool will be divided into $G = 3$ groups each having two sequences.

$$\mathbf{S} = \frac{1}{\sqrt{8}} \begin{bmatrix} -1-i & -1+i & -1+i & 1+i & -1+i & 1-i \\ -1+i & 1-i & 1+i & -1+i & -1-i & -1+i \\ -1+i & -1+i & 1-i & 1-i & -1-i & 1+i \\ 1+i & -1-i & -1+i & -1+i & -1-i & -1-i \end{bmatrix}. \quad (18)$$

Algorithm 3 Sequence grouping for small power offset

```

1: Let  $g = 1$  and  $\mathbf{S}^{(1)} = \mathbf{S}$ . // Initialization
2: loop
3:   if  $g < G$  then
4:     Compute matrix  $\mathbf{C} = |(\mathbf{S}^{(g)})^H \mathbf{S}^{(g)}|$ .
       // Cross-correlation matrix
5:     Compute vector  $\mathbf{c} = \left[ \sum_{j=1}^{L-\sum_{m=1}^{g-1} L_m} \mathbf{C}_{1j}^2, \dots, \right.$ 
        $\left. \sum_{j=1}^{L-\sum_{m=1}^{g-1} L_m} \mathbf{C}_{(L-\sum_{m=1}^{g-1} L_m)j}^2 \right]$ .
       // Sum cross-correlations of sequences in groups
       // with the same or lower powers
6:     Find the  $L_g$  smallest values in  $\mathbf{c}$  and denote the
       index set as  $\mathcal{I}_g$ .
       // Find sequences index for group  $g$ 
7:     Define  $\mathbf{S}_g = [\mathbf{S}^{(g)}]_{\mathcal{I}_g}$  as sequences for group  $g$ ,
       where  $[\cdot]_j$  denotes the  $j^{\text{th}}$  column of a matrix.
       // Find the optimal sequences for group  $g$ 
8:     Update  $g = g + 1$  and  $\mathbf{S}^{(g)} = \mathbf{S}^{(g-1)} \setminus \mathbf{S}_{g-1}$ .
9:   end if
10: end loop

```

1. Large power offset

There are $\binom{6}{2} = 15$ combinations of the two sequences for group 1. First, compute the TSC of sequences for all the 15 combinations. Second, find the minimum TSC in the 15 combinations and define the corresponding sequences as the sequences for group 1. These are

$$\mathbf{S}_1 = \frac{1}{\sqrt{8}} \begin{bmatrix} -1-i & 1-i \\ -1+i & -1+i \\ -1+i & 1+i \\ 1+i & -1-i \end{bmatrix}. \quad (19)$$

Then update the sequence pool with the remaining four sequences as

$$\mathbf{S}^{(2)} = \frac{1}{\sqrt{8}} \begin{bmatrix} \underbrace{-1+i \ -1+i}_{\mathbf{S}_2 \text{ for group 2}} & \underbrace{1+i \ -1+i}_{\mathbf{S}_3 \text{ for group 3}} \\ \underbrace{1-i \ 1+i}_{\mathbf{S}_2 \text{ for group 2}} & \underbrace{-1+i \ -1-i}_{\mathbf{S}_3 \text{ for group 3}} \\ \underbrace{-1+i \ 1-i}_{\mathbf{S}_2 \text{ for group 2}} & \underbrace{1-i \ -1-i}_{\mathbf{S}_3 \text{ for group 3}} \\ \underbrace{-1-i \ -1+i}_{\mathbf{S}_2 \text{ for group 2}} & \underbrace{-1+i \ -1-i}_{\mathbf{S}_3 \text{ for group 3}} \end{bmatrix}. \quad (20)$$

Find all the $\binom{4}{2} = 6$ combinations of two sequences in Eq. (20) for group 2. Compute TSC of the sequences in the six combinations respectively and find the combination with the minimum TSC as the sequences for group 2. Finally, the remaining two sequences are for group 3 as given in Eq. (20).

2. Small power offset

First, compute the sum cross-correlations of Eq. (18) as $\mathbf{c} = [1.5, 2, 2, 2.25, 1.75, 2]$. Second, find the index set with two smallest sum cross-correlations, which is $\mathcal{I}_1 = \{1, 5\}$. The sequences

of group 1 are given as

$$\mathbf{S}_1 = \frac{1}{\sqrt{8}} \begin{bmatrix} -1-i & -1+i \\ -1+i & 1-i \\ -1+i & -1+i \\ 1+i & -1-i \end{bmatrix}. \quad (21)$$

Then update the sequence pool with the remaining four sequences as

$$\mathbf{S} = \frac{1}{\sqrt{8}} \begin{bmatrix} \underbrace{-1+i \ -1+i}_{\mathbf{S}_2 \text{ for group 2}} & \underbrace{1+i \ 1-i}_{\mathbf{S}_3 \text{ for group 3}} \\ \underbrace{1-i \ 1+i}_{\mathbf{S}_2 \text{ for group 2}} & \underbrace{-1+i \ -1+i}_{\mathbf{S}_3 \text{ for group 3}} \\ \underbrace{-1+i \ 1-i}_{\mathbf{S}_2 \text{ for group 2}} & \underbrace{1-i \ 1+i}_{\mathbf{S}_3 \text{ for group 3}} \\ \underbrace{-1-i \ -1+i}_{\mathbf{S}_2 \text{ for group 2}} & \underbrace{-1+i \ -1-i}_{\mathbf{S}_3 \text{ for group 3}} \end{bmatrix}. \quad (22)$$

Compute the sum cross-correlations of the remaining four sequences as $\mathbf{c} = [1.625, 1.875, 1.875, 1.875]$. Find the index set with two smallest sum cross-correlations. This is $\mathcal{I}_2 = \{1, 2\}$. The sequences of groups 2 and 3 are given in Eq. (22).

3.4 Performance and complexity analysis

From the analysis in Sections 3.2 and 3.3, we find that the proposed NOMA enhancements are independent of the sequence design and can be combined with any sequence-based NOMA scheme for performance enhancement. Multi-level received powers can always help facilitate SIC receiving and hence promote performance. However, the performance gain of sequence grouping depends on the sequence pools.

1. WBE and Grassmannian sequences

The cross-correlations and sum cross-correlations are close and identical to each other for WBE and Grassmannian sequences, respectively. This indicates that sequence grouping has little performance gain for sequence-based NOMA with WBE and Grassmannian sequences.

2. Random complex sequences

Random complex sequences are less designed and hence have large and diverse cross-correlations. Sequence grouping in this case can achieve a large performance gain.

3. ZC sequences

Based on the properties of ZC sequences in Section 2.2, sequences with one root can be allocated into one group. This is the same as Teng et al. (2017). The difference from Teng et al. (2017) is that the number of sequences in one group is not limited by the number of CSs; i.e., sequences with different roots may be allocated to one group and sequences with one root may be allocated into multiple groups

if the user number in one group is larger or smaller than the number of CSs, respectively, which indicates that the sequence grouping proposed in Section 3.3 is much more flexible.

4. GWBE sequences

To maximize the ergodic sum capacity, GWBE sequences for users with larger power are designed with lower sum cross-correlations, while the sequences for users with lower power are designed with higher sum cross-correlations. This coincides with our motivation of sequence grouping and can further enhance performance. Note that GWBE sequences are designed for received power $\{\tilde{P}_1, \tilde{P}_2, \dots, \tilde{P}_G\}$ and sequence grouping is not necessary.

The transceiver structure of NOMA with user grouping is given in Fig. 3, where multi-level received powers and sequences for each group are all pre-defined at the users and BSs. Therefore, sequence grouping in Algorithms 2 and 3 will not increase the complexity at the transmitter. This is identical with existing sequence-based NOMA schemes.

At the receiver, a minimum mean squared error (MMSE)-SIC receiver can be used, where users are first ordered based on instantaneous received powers or SINR and then detected based on the order (Fig. 3). Under AWGN channels, the instantaneous received power is the same as the average received power \tilde{P}_g . User groups will be detected successively, while users in each group are detected, rebuilt, and deleted in parallel. Under fading channels, the instantaneous received powers of multiple users will depend not only on average power \tilde{P}_g but also on the power of the instantaneous fading channel. In this case, the detection order is independent of the user groups and a typical MMSE-SIC receiver can be used. The MMSE detector for user n_k is

$$\mathbf{w}_{n_k} = \left(\sum_{i=k}^K \tilde{\mathbf{h}}_{n_i} \tilde{\mathbf{h}}_{n_i}^H + \sigma^2 \mathbf{I} \right)^{-1} \tilde{\mathbf{h}}_{n_k}, \quad (23)$$

where $\tilde{\mathbf{h}}_{n_i} = [(\mathbf{h}_{1,n_i} \circ \mathbf{s}_{n_i})^H, \dots, (\mathbf{h}_{N_{\text{Rx}},n_i} \circ \mathbf{s}_{n_i})^H]^H \in \mathbb{C}^{N_{\text{Rx}} \times 1}$ denotes the effective channel vector of user n_i , N_{Rx} denotes the number of receive antennas at the BS, $\mathbf{h}_{m,n_i} \in \mathbb{C}^{N \times 1}$ is the channel of user n_i at the m^{th} antenna, and ‘ \circ ’ is element-wise multiplication.

Then the complexity is dominated by matrix inversion in Eq. (23) with dimension $N_{\text{Rx}}N \times N_{\text{Rx}}N$ and the complexity order is $\mathcal{O}(KN_{\text{Rx}}^3N^3)$, which increases linearly with the number of users.

Table 2 Simulation parameters

Parameter	Value or assumption
Carrier frequency	2 GHz
Waveform	CP-OFDM
Numerology	SCS = 15 kHz
Number of UEs	16
Number of BS antennas	2
Channel model	TDL-C with 300 ns delay spread (3GPP, 2017c)
Channel estimation	Ideal
Signature allocation	Fixed
Channel coding	Turbo
Allocated bandwidth	4 RB for NOMA 1 RB for OMA
Modulation	QPSK for NOMA 64QAM for OMA
Code rate	1/2 for NOMA 2/3 for OMA

4 Simulation results

In this section, link-level simulations are performed to evaluate the performance of the proposed sequence design and NOMA schemes. The number of users is 16 and the spectral efficiency (SE) target per user is 0.25 bits/(s · Hz). Random complex sequences in 3GPP (2017a) and WBE sequences with length 4 are considered; i.e., the spreading factor is 4 and the overloading factor is 400%. The MMSE-SIC receiver in Fig. 3 and Eq. (23) is employed. The SIC order is decided by the instantaneous channel power. The transmission bandwidth is 4 resource blocks (RB) and the time-frequency resources of DMRS are the same as the LTE uplink, i.e., 2 DMRS symbols per RB and the overhead is 1/7. The performance of OMA is evaluated. For fair comparison, the total average received powers of users in NOMA with equal and unequal average received powers are identical, and the total SEs of NOMA and OMA are identical. The detailed parameters are listed in Table 2.

4.1 Fixed signature allocation

4.1.1 Impacts of sequence design

In Fig. 4, the performance of four sequence pools—random complex sequences, WBE sequences with $L = 8$ and $L = 16$, and GWBE sequences—are compared under different power offsets. Under equal received power ($G = 1$ and $\text{PO} = 0$ dB), the schemes with random complex sequences and WBE sequences reduce to MUSA and WSMA, respectively. For better understanding, we use sequence types instead of

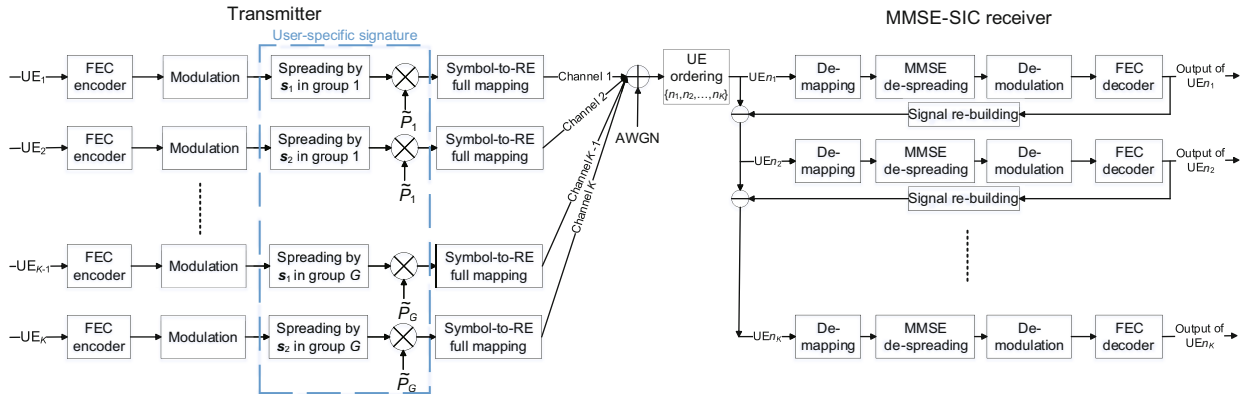


Fig. 3 Transceiver of non-orthogonal multiple access with user grouping

NOMA schemes for comparison in this subsection. We find that under equal received power $G = 1$ and $PO = 0$ dB, the block error rate (BLER) of WBE sequences with $L = 16$ is much lower than that of random complex sequences, and 2.5 dB signal-to-noise ratio (SNR) gain at 0.1 BLER target is achieved. This is consistent with the conclusion in Section 2.2 that WBE sequences are the optimal.

For unequal received power, i.e., $PO = 5$ dB for two groups, the performances of the four pools reduce in the order of GWBE sequences, WBE sequences with $L = 16$, random complex sequences, and WBE sequences with $L = 8$. This indicates that first the proposed GWBE sequences under unequal received power are the optimal and the performance gain is large especially when BLER is low. Second, reusing the WBE sequences with $L = 8$ in the two groups performs worse than allocating the WBE se-

quences with $L = 16$ into the two groups. This is consistent with the analysis in Section 2.2.2. In other words, employing received power as the only MA signature, such as DMRS-staggered NCMA in 3GPP (2016m), performs worse than employing both received power and non-orthogonal sequences as the MA signature to distinguish users at the receiver, such as in the proposed NOMA scheme with user grouping in Section 3.

4.1.2 Impact of multi-level received powers

To validate the impact of multi-level received powers, the performance of NOMA with different power offsets and grouping number under random complex sequences without sequence grouping is shown in Fig. 5.

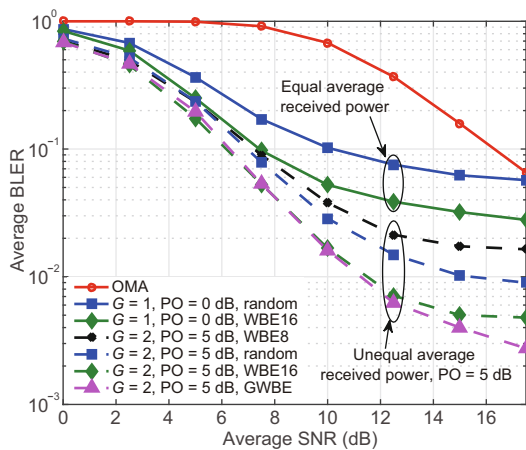


Fig. 4 Average block error rate (BLER) under different sequence pools and power offset (PO)

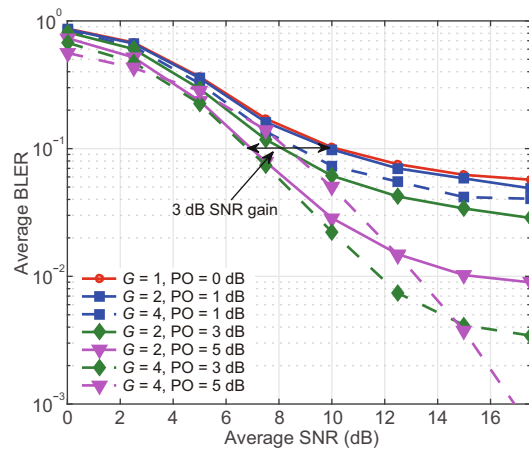


Fig. 5 Average block error rate (BLER) under different power offsets (POs) and grouping number G . Random complex sequences without sequence grouping are used

From Fig. 5, we find that for $G = 2$, i.e., two power levels, BLER reduces with the increase of power offset. This indicates that a larger power offset will help reduce inter-group interference and hence enhance the performance. While for $G = 4$, i.e., four power levels, when the average SNR is larger than 15 dB, the BLER reduces with the power offset. However, when the average SNR is smaller than 15 dB, BLER first reduces and then increases with power offset. The reason is that to maintain the same average SNR, received power of the group with lowest SIC order decreases with the group number G and power offset. This will lead to poor performance even if error propagation is very small.

Similarly, when the power offset is small, such as 1 dB and 3 dB, the received power of the 4th group in NOMA with $G = 4$ is not very low, and MUI dominates the performance. Therefore, NOMA with $G = 4$ achieves better performance than NOMA with $G = 2$. While for large power offset, such as 5 dB, the received power of the 4th group in NOMA with $G = 4$ is extremely low in the region of low average SNR and dominates the performance. This results in worse performance than NOMA with $G = 2$.

The same results for random complex sequences in Fig. 5 can be observed for WBE sequences with $L = 16$ and GWBE sequences as in Figs. 6 and 7, respectively. This indicates that NOMA with multi-level received powers can always enhance the performance of sequence-based NOMA schemes with any sequence pool. However, considering that the average BLER is either dominated by the lowest received power or by the MUI, the optimal number of power levels G and power offset should be selected based on the average SNR and BLER requirement.

4.1.3 Impact of sequence grouping

The impact of sequence grouping on BLER is given in Figs. 8 and 9 for random complex sequences and WBE sequences, respectively.

For random complex sequences in Fig. 8, we find that sequence grouping based on Algorithm 2 for large power offset and Algorithm 3 for small power offset can always enhance the performance of random complex sequences. The SNR gain increases with the reduction of BLER; i.e., the proposed NOMA scheme can enhance the performance especially in the scenarios with a high reliability requirement.

For WBE sequences in Fig. 9, sequence grouping

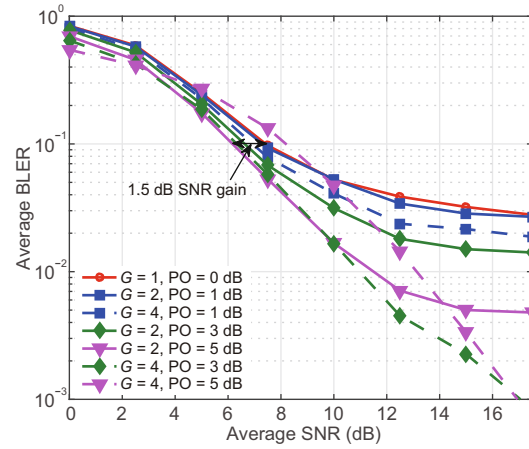


Fig. 6 Average block error rate (BLER) under different power offsets (POs) and grouping number G . WBE sequences ($L = 16$) without sequence grouping are used

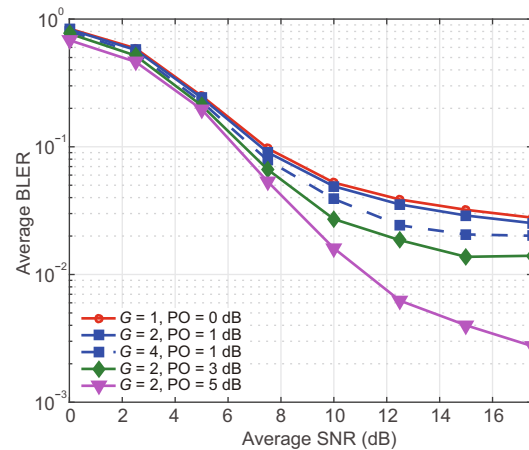


Fig. 7 Average block error rate (BLER) under different power offsets (POs) and grouping number G . GWBE sequences without sequence grouping are used

has nearly no performance gain, which is consistent with the analysis in Section 3.4.

Furthermore, we find that the proposed NOMA scheme can achieve more than 10 dB SNR gain at 0.1 BLER target compared with OMA for both random complex sequences and WBE sequences. In addition, the proposed NOMA scheme can achieve a lower BLER requirement such as 0.01 when existing NOMA schemes have error floors.

To validate the impact of the channel model, the performance under TDL-A channel with 30 ns delay spread (3GPP, 2017c) and random complex sequences is provided in Fig. 10. Under TDL-A channel, 4.2 dB SNR gain over NOMA without user

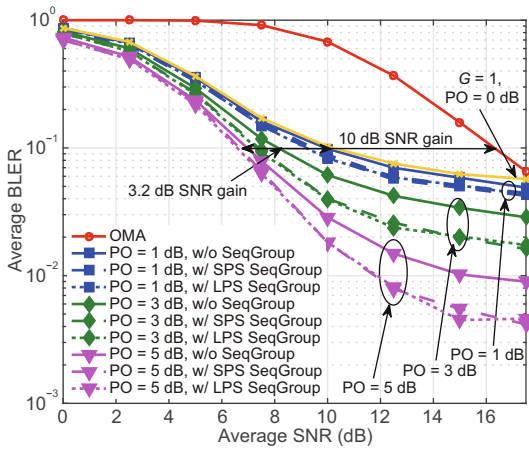


Fig. 8 Average block error rate (BLER) under different power offsets and sequence grouping methods. Random complex sequences are used. ‘LPS’ and ‘SPS’ denote large and small power offsets, respectively

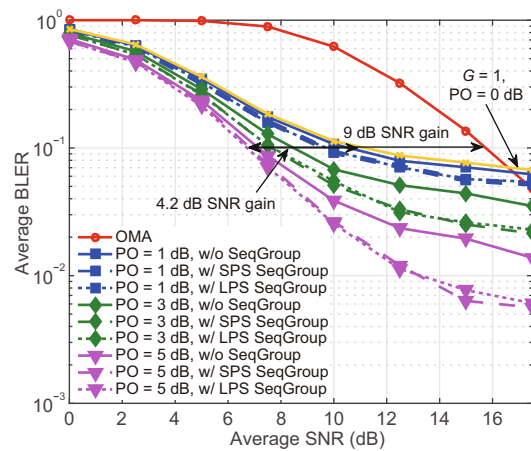


Fig. 10 Average block error rate (BLER) under different power offsets and sequence grouping methods. Random complex sequences and TDL-A channel with 30 ns delay spread are considered

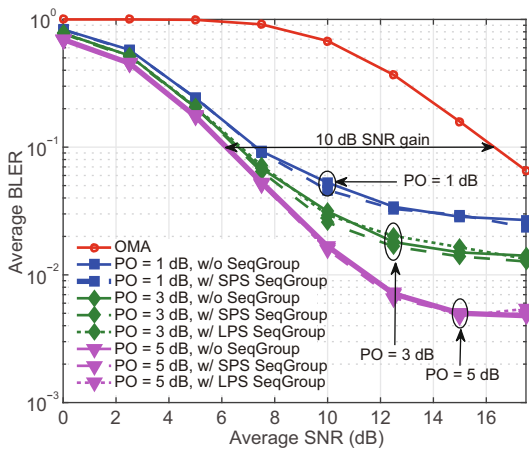


Fig. 9 Average block error rate (BLER) under different power offsets and sequence grouping methods. WBE sequences are used

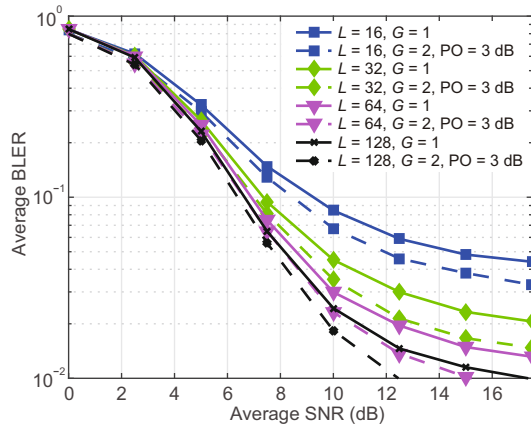


Fig. 11 Average block error rate (BLER) under different number of WBE sequences and groups. Random signature selection is used. TDL-C channel with 300 ns delay spread is considered

grouping, i.e., $G = 1$ and $PO = 0$ dB, can be achieved. This is larger than the 3.2 dB gain in the TDL-C channel. This indicates that the proposed schemes perform better under flatter channels.

4.2 Random signature selection

To verify the impact of signature collision in grant-free transmission, NOMA with random signature selection is evaluated in Fig. 11. For NOMA with multi-level received powers, a set composed of power and sequence is defined as a signature. To reduce collision, the sequence pool is reused in all user groups; i.e., if G multi-level powers are considered and the size of the sequence pool is L , the size of the

signature pool becomes GL . Then it shows that the case of $L = 16$ and $G = 2$ has the same number of signatures as the case of $L = 32$ and $G = 1$.

From Fig. 11, it can be observed that for a given number of users, BLER reduces with the number of sequences and signatures. This indicates that a large number of signatures can reduce the collision probability and hence enhance the performance. In addition, for any L , NOMA with multi-level received powers (i.e., $G = 2$ in Fig. 11) can achieve better BLER performance than conventional NOMA (i.e., $G = 1$). This indicates that multi-level received powers (i.e., NOMA with user grouping) can increase the signature pool size and enhance the performance under random signature selection.

5 Conclusions

We have proposed to use power as part of the MA signature. Based on unequal received power, three enhancements for uplink NOMA have been investigated. First, we have proposed the optimal sequence design, i.e., GWBE sequences, for sequence-based NOMA schemes. Then to facilitate SIC receiving, we have proposed user grouping with multi-level received powers, where users in one group have the same received power and users in different groups have different received powers. Then sequence grouping based on cross-correlations has been proposed and the grouping algorithms for different power offsets have been discussed. The evaluation results based on link-level simulations showed that the proposed GWBE sequences can achieve lower BLER than sequences in existing NOMA schemes and the gain is large especially when BLER is very low. For the system with 400% overloading and fixed signature allocation, NOMA with proposed enhancements can achieve 0.01 BLER while existing NOMA schemes have error floors. This showed that larger connectivity and higher reliability can be achieved by the proposed schemes. At the 0.1 BLER target, the proposed enhancements with multi-level received powers and sequence grouping can achieve more than 3 dB and 10 dB SNR gains over conventional NOMA and OMA, respectively. For random signature allocation, NOMA with multi-level powers can reduce collision probability and enhance the performance. This is promising for systems of 5G and beyond.

References

- 3GPP, 2012. Physical channels and modulation (Release 11). Technical Report, TS-36.211.
- 3GPP, 2015. Study on downlink multiuser superposition transmission (MUST) for LTE (Release 13). Technical Report, TR-36.859. Belgrade, Serbia.
- 3GPP, 2016a. Sparse code multiple access (SCMA) for 5G radio transmission. Technical Report, TR1-162155. Busan, Korea.
- 3GPP, 2016b. Candidate new radio multiple access schemes. Technical Report, TR1-162202. Busan, Korea.
- 3GPP, 2016c. Discussion on multiple access for new radio interface. Technical Report, TR1-162226. Busan, Korea.
- 3GPP, 2016d. Candidate solution for new multiple access. Technical Report, TR1-162306. Busan, Korea.
- 3GPP, 2016e. Multiple access schemes for new radio interface. Technical Report, TR1-162385. Busan, Korea.
- 3GPP, 2016f. Considerations on downlink/uplink multiple access for new radio. Technical Report, TR1-162517. Busan, Korea.
- 3GPP, 2016g. Non-orthogonal multiple access candidate for new radio. Technical Report, TR1-163992. Nanjing, China.
- 3GPP, 2016h. Initial link-level simulation results for uplink non-orthogonal multiple access. Technical Report, TR1-164329. Nanjing, China.
- 3GPP, 2016i. Low code rate and signature based multiple access scheme for new radio. Technical Report, TR1-164869. Nanjing, China.
- 3GPP, 2016j. Non-orthogonal multiple access for new radio. Technical Report, TR1-165019. Nanjing, China.
- 3GPP, 2016k. Performance of interleave division multiple access (IDMA) in combination with OFDM family waveforms. Technical Report, TR1-165021. Nanjing, China.
- 3GPP, 2016l. On uplink non-orthogonal multiple access schemes. Technical Report, TR1-166552. Gothenburg, Sweden.
- 3GPP, 2016m. Non-orthogonal multiple access scheme based on non-orthogonal coded multiple access. Technical Report, TR1-166871. Gothenburg, Sweden.
- 3GPP, 2016n. Discussion on multiple access for uplink machine type communications. Technical Report, TR1-167392. Gothenburg, Sweden.
- 3GPP, 2016o. New uplink non-orthogonal multiple access schemes for new radio. Technical Report, TR1-167535. Gothenburg, Sweden.
- 3GPP, 2017a. Link-level simulation and preliminary performance comparison of non-orthogonal multiple access schemes. Technical Report, TR1-1720222. Reno, USA.
- 3GPP, 2017b. Study on new radio access technology physical layer aspects (Release 14). Technical Report, TR-38.802.
- 3GPP, 2017c. Study on channel model for frequencies from 0.5 to 100 GHz (Release 14). Technical Report, TR-38.901.
- Andrews JG, Buzzi S, Choi W, et al., 2014. What will 5G be? *IEEE J Sel Areas Commun*, 32(6):1065-1082. <https://doi.org/10.1109/JSAC.2014.2328098>
- Chen S, Ren B, Gao Q, et al., 2017. Pattern division multiple access—a novel nonorthogonal multiple access for the fifth-generation radio networks. *IEEE Trans Veh Technol*, 66(4):3185-3196. <https://doi.org/10.1109/TVT.2016.2596438>
- Chen X, Benjebbour A, Li A, et al., 2014. Multi-user proportional fair scheduling for uplink non-orthogonal multiple access (NOMA). 79th IEEE Conf on Vehicular Technology, p.1-5. <https://doi.org/10.1109/VTCSpring.2014.7022998>
- Dahlman E, Mildh G, Parkvall S, et al., 2014. 5G wireless access: requirements and realization. *IEEE Commun Mag*, 52(12):42-47. <https://doi.org/10.1109/MCOM.2014.6979985>
- Dai L, Wang B, Yuan Y, et al., 2015. Non-orthogonal multiple access for 5G: solutions, challenges, opportunities, and future research trends. *IEEE Commun Mag*, 53(9):74-81. <https://doi.org/10.1109/MCOM.2015.7263349>
- Datta S, Howard S, Cochran D, 2012. Geometry of the Welch bounds. *Linear Algebra & Its Appl*, 437(10):2455-2470. <https://doi.org/10.1016/j.laa.2012.05.036>

- Dhillon IS, Heath RW, Sustik MA, et al., 2005. Generalized finite algorithms for constructing Hermitian matrices with prescribed diagonal and spectrum. *SIAM J Matr Anal Appl*, 27(1):61-71. <https://doi.org/10.1137/S0895479803438183>
- Ding Z, Adachi F, Poor HV, 2016a. The application of MIMO to non-orthogonal multiple access. *IEEE Trans Wirel Commun*, 15(1):537-552. <https://doi.org/10.1109/TWC.2015.2475746>
- Ding Z, Fan P, Poor HV, 2016b. Impact of user pairing on 5G nonorthogonal multiple-access downlink transmissions. *IEEE Trans Veh Technol*, 65(8):6010-6023. <https://doi.org/10.1109/TVT.2015.2480766>
- Endo Y, Kishiyama Y, Higuchi K, 2012. Uplink non-orthogonal access with MMSE-SIC in the presence of inter-cell interference. *Int Symp on Wireless Communication Systems*, p.261-265. <https://doi.org/10.1109/ISWCS.2012.6328370>
- Guess T, Varanasi M, 2000. Error exponents for maximum-likelihood and successive decoders for the Gaussian CDMA channel. *IEEE Trans Inform Theory*, 46(4):1683-1691. <https://doi.org/10.1109/18.850716>
- Islam SMR, Avazov N, Dobre OA, et al., 2017a. Power-domain non-orthogonal multiple access (NOMA) in 5G systems: potentials and challenges. *IEEE Commun Surv Tutor*, 19(2):721-742. <https://doi.org/10.1109/COMST.2016.2621116>
- Islam SMR, Zeng M, Dobre OA, 2017b. Non-orthogonal multiple access in 5G systems: exciting possibilities for enhancing spectral efficiency. <https://arxiv.org/abs/1706.08215>
- ITU-R, 2015. IMT vision—framework and overall objectives of the future development of IMT for 2020 and beyond. Technical Report, M.2083-0.
- Li A, Chen X, Jiang H, 2017. Contention based uplink transmission with non-orthogonal multiple access for latency reduction. 85th IEEE Conf on Vehicular Technology, p.1-6. <https://doi.org/10.1109/VTCSpring.2017.8108486>
- Li L, Goldsmith A, 2001. Capacity and optimal resource allocation for fading broadcast channels. I. Ergodic capacity. *IEEE Trans Inform Theory*, 47(3):1083-1102. <https://doi.org/10.1109/18.915665>
- Massey JL, Mittelholzer T, 1993. Welch's Bound and Sequence Sets for Code-Division Multiple-Access Systems. Springer, New York, USA.
- Medra A, Davidson TN, 2014. Flexible codebook design for limited feedback systems via sequential smooth optimization on the Grassmannian manifold. *IEEE Trans Signal Process*, 62(5):1305-1318. <https://doi.org/10.1109/TSP.2014.2301137>
- Nagata S, Wang L, Takeda K, 2017. Industry perspectives. *IEEE Wirel Commun*, 24(3):2-4. <https://doi.org/10.1109/MWC.2017.7955902>
- Nikopour H, Baligh H, 2013. Sparse code multiple access. 24th Int Symp on Personal Indoor and Mobile Radio Communications, p.332-336. <https://doi.org/10.1109/PIMRC.2013.6666156>
- Osseiran A, Boccardi F, Braun V, et al., 2014. Scenarios for 5G mobile and wireless communications: the vision of the METIS project. *IEEE Commun Mag*, 52(5):26-35. <https://doi.org/10.1109/MCOM.2014.6815890>
- Ping L, Liu L, Wu K, et al., 2006. Interleave division multiple access. *IEEE Trans Wirel Commun*, 5(4):938-947. <https://doi.org/10.1109/TWC.2006.1618943>
- Saito Y, Kishiyama Y, Benjebbour A, et al., 2013. Non-orthogonal multiple access (NOMA) for cellular future radio access. 77th IEEE Conf on Vehicular Technology, p.1-5. <https://doi.org/10.1109/VTCSpring.2013.6692652>
- She C, Yang C, Quek TQS, 2017. Radio resource management for ultra-reliable and low-latency communications. *IEEE Commun Mag*, 55(6):72-78. <https://doi.org/10.1109/MCOM.2017.1601092>
- Sun Q, Han S, Chin-Lin I, et al., 2015. On the ergodic capacity of MIMO NOMA systems. *IEEE Wirel Commun Lett*, 4(4):405-408. <https://doi.org/10.1109/LWC.2015.2426709>
- Taherzadeh M, Nikopour H, Bayesteh A, et al., 2014. Sparse code multiple access codebook design. 80th IEEE Conf on Vehicular Technology, p.1-5. <https://doi.org/10.1109/VTCSFall.2014.6966170>
- Teng CF, Liao CC, Cheng HY, et al., 2017. Reliable compressive sensing (CS)-based multi-user detection with power-based Zadoff-Chu sequence design. *IEEE Int Workshop on Signal Processing Systems*, p.1-5. <https://doi.org/10.1109/SiPS.2017.8110015>
- Tse D, Viswanath P, 2015. Fundamentals of Wireless Communication. Cambridge University Press, Cambridge, UK. <https://doi.org/10.1017/CBO9780511807213>
- Viswanath P, Anantharam V, 1999. Optimal sequences and sum capacity of synchronous CDMA systems. *IEEE Trans Inform Theory*, 45(6):1984-1991. <https://doi.org/10.1109/18.782121>
- Viswanath P, Anantharam V, Tse D, 1999. Optimal sequences, power control, and user capacity of synchronous CDMA systems with linear MMSE multi-user receivers. *IEEE Trans Inform Theory*, 45(6):1968-1983. <https://doi.org/10.1109/18.782119>
- Wang C, Chen Y, Wu Y, et al., 2017. Performance evaluation of grant-free transmission for uplink URLLC services. 85th IEEE Conf on Vehicular Technology, p.1-6. <https://doi.org/10.1109/VTCSpring.2017.8108593>
- Welch L, 1974. Lower bounds on the maximum cross correlation of signals (Corresp). *IEEE Trans Inform Theory*, 20(3):397-399. <https://doi.org/10.1109/TIT.1974.1055219>
- Wu Y, Zhang S, Chen Y, 2015. Iterative multiuser receiver in sparse code multiple access systems. *IEEE Int Conf on Communications*, p.2918-2923. <https://doi.org/10.1109/ICC.2015.7248770>
- Yuan Z, Yu G, Li W, et al., 2016. Multi-user shared access for Internet of Things. 83rd IEEE Conf on Vehicular Technology, p.1-5. <https://doi.org/10.1109/VTCSpring.2016.7504361>
- Zeng M, Yadav A, Dobre OA, et al., 2017a. Capacity comparison between MIMO-NOMA and MIMO-OMA with multiple users in a cluster. *IEEE J Sel Areas Commun*, 35(10):2413-2424. <https://doi.org/10.1109/JSAC.2017.2725879>
- Zeng M, Yadav A, Dobre OA, et al., 2017b. On the sum rate of MIMO-NOMA and MIMO-OMA systems. *IEEE Wirel Commun Lett*, 6(4):534-537. <https://doi.org/10.1109/LWC.2017.2712149>